
QUANTITATIVE AND QUALITATIVE COMPARISON OF GENERATIVE MODELS FOR SUBJECT-SPECIFIC GAZE SYNTHESIS: DIFFUSION VS GAN

Kamrul Hasan¹, Dmytro Katrychuk¹, Mehedi Hasan Raju¹, Oleg V. Komogortsev¹

¹Texas State University, San Marcos, Texas, USA

{kamrul.hasan, d_k139, m.raju, ok}@txstate.edu

ABSTRACT

Recent advances in deep learning demonstrate the ability to generate synthetic gaze data. However, most approaches have primarily focused on generating data from random noise distributions or global, predefined latent embeddings, whereas individualized gaze sequence generation has been less explored. To address this gap, we revisit two recent approaches based on diffusion and generative adversarial networks (GANs) and introduce modifications that make both models explicitly subject-aware while improving accuracy and effectiveness. For the diffusion-based approach, we utilize compact user embeddings that emphasize per-subject traits. Moreover, for the GAN-based approach, we propose a subject-specific synthesis module that conditioned the generator to retain better idiosyncratic gaze information. Finally, we conduct a comprehensive assessment of these modified approaches utilizing standard eye-tracking signal quality metrics, including spatial accuracy and precision. This work helps define synthetic signal quality, realism, and subject specificity, thereby contributing to the potential development of gaze-based applications.

Keywords Eye tracking, Subject-specific Gaze Synthesis, Diffusion, Generative Adversarial Networks, Synthetic Eye Movement, Privacy-preserving Biometrics

1 Introduction

Eye-tracking research has gained substantial momentum with recent advances in technology that enable the convenient and high-quality capture of gaze data [1–3]. Adding these technological advances to methodological advancements has expanded the field’s influence across various domains [4]. This progress is evident in healthcare—where eye movements facilitate dyslexia identification [5] and autism spectrum disorder (ASD) detection [6]—as well as evaluation and security, where gaze behavior enables user authentication [7, 8] and liveness detection through distinctive dynamics of eye movement [9, 10]. In addition to these domains, eye-tracking facilitates foveated rendering [11] in augmented and virtual reality (AR/VR), enhances adaptive interfaces [12], and supports attention-aware tutoring [13]. These applications and developments highlight eye movement as an informative signal and eye-tracking as a versatile tool for both clinical insights and robust, privacy-aware human–computer interaction (HCI).

However, to make these applications a reality, high-sampling-rate (e.g., 250–1000 Hz) eye trackers [14] are a key component, which record micro oculomotor events (such as microsaccades and fine-grained smooth pursuit) and extract subject-specific patterns that are not as precise at lower sample rates (e.g., 30–60 Hz). Previous studies [15–17] have shown that shorter segments of high-sampling-rate recordings can compete with, or even surpass, longer and lower-sampling-rate sequences in tasks such as gaze-based user authentication [7]. It underscores that gaze data carries significant biometric and behavioral features. In addition, high-frequency gaze sequences have detailed subject-specific information that can enable re-identification [18] and the inference of sensitive attributes (e.g., gender, identity, ethnicity), raising significant privacy concerns [19]. However, the limited availability of high-quality public datasets remains a significant bottleneck for advancing the field. Collecting large, diverse, and high-quality eye-tracking data is equipment- and labor-intensive [3], requires controlled protocols, lengthy recording sessions, and often demands expert

annotation of oculomotor events. These constraints warrant reducing reliance on real data but focusing on subject-aware synthetic data generation while preserving the properties required.

Synthetic data generation is emerging as a promising solution to address data shortages and mitigate privacy concerns [20]. Early simulators and statistical measures [21, 22] primarily generated fixation positions and durations or relied on simplified parametric procedures that constrain realism and subject specificity. More recently, with the wider adoption of generative adversarial networks (GANs) [23], SP-EyeGAN [24] has been used to produce realistic temporal scanpaths, including both fixations and saccades, and these synthetic data have been employed for pre-training to conduct downstream tasks. However, they use a random noise distribution to generate signals that are not specific to the target, which limits the approach’s practicality in real applications. Later, denoising diffusion probabilistic models (DDPMs) [25] have introduced strong priors for time-series generation; DiffEyeSyn [26], in particular, conditions a diffusion process on identity-removed signals and user embeddings to inject user-specific attributes while preserving natural gaze trajectory. These advances motivate a systematic study of how to best encode subject identity and which generative approach most effectively preserves individual gaze behavior.

Building on these foundations, we instantiate subject-specific variants of both generative approaches. In terms of diffusion, we adhere to DiffEyeSyn’s [26] approach, introducing two specific modifications. First, we derive the conditional signal by downsampling to 25 Hz and then upsampling to the raw rate (i.e., 1000 Hz), motivated by evidence that subject identity above low frequencies can be removed without discarding task-relevant kinematics [27]. Secondly, we substitute the 512-dimensional conditioning vector with a concise 128-dimensional user embedding. Collectively, these modifications yield more authentic, subject-specific synthetic gaze signals. Similarly, in the GAN-based approach, we enhanced SP-EyeGAN’s [24] dual generators for fixations and saccades by incorporating a Subject-Specific Condition Generator (SCG) module with two branches. The first branch—Directional Data Quality Feature Extractor (DDQFE)—compacts velocity signals into displacement profiles while extracting spatial dispersion (i.e., standard deviation) and temporal significance (i.e., root-mean-square error). The second branch encodes subject identity through a one-hot (OH) encoding representation. Subsequently, the SCG module concatenates the DDQFE features with the OH vector, integrates them with the latent noise, and then passes the resulting features through the generators. This quality-aware conditioning improves authenticity and subject specificity while maintaining a lightweight structure.

Finally, we conduct a rigorous head-to-head evaluation of the revised diffusion and GAN-based approach under the same setting. We report standard signal-quality metrics, including spatial accuracy and spatial precision, with a user-centric evaluation strategy ([28]). Additionally, we also report cosine similarity between embeddings from synthetic and real signals.

Overall, the specific contributions of our work are twofold:

1. A compact-embedding and identity-removed signal conditioning variant of DiffEyeSyn that improves subject specificity with lower complexity. Additionally, an enhanced SP-EyeGAN with an explicit Subject-Specific Condition Generator that fuses DDQFE’s features with one-hot encoding subject identity to guide realistic fixation and saccade generation.
2. A qualitative and quantitative comparison of the above-mentioned approaches for subject-specific gaze synthesis.

2 Related Work

2.1 Statistical Models

Earlier models for eye movement synthesis relied primarily on training-free statistical methods grounded in signal processing [21, 29, 30]. As such, approaches ranging from saccade-based animation [21] and head–gaze coordination [31] to photorealistic image generation with SynthesEyes [32] were used to model realistic eye movements and gaze behavior. While these studies established foundational realism, they did not capture the full complexity of human oculomotor behavior.

Subsequent statistical models [22, 33–36] advanced gaze synthesis by integrating known oculomotor characteristics. EyeCatch [36] used a Kalman filter [37] to simulate fixations, saccades, and smooth pursuits. EyeSyn [22] further introduced a physics-based framework that models these movements with psychology-inspired equations and adds realistic jitter through Gaussian drift and pink noise. Despite these advances, training-free methods still yield average behavior, overlook individual variability, and simplify eye movements, such as microsaccades and tremors. Consequently, data-driven machine learning approaches are increasingly adopted to model individualized gaze dynamics.

2.2 Machine-learning Models

To address the limitations of statistical models in synthetic data generation, researchers have recently concentrated on machine learning approaches, particularly deep neural networks [17, 23, 38–40]. Initial research integrated visual inputs with sequence models to predict human-like scanpaths. Simon et al. [38] employed a CNN-LSTM architecture that takes a static image and generates a realistic eye-tracking sequence (a series of fixations and saccades), thereby learning typical human scanning patterns. Similarly, Assens et al. [39] proposed PathGAN, which comprises GANs that output likely fixation points on an image. PathGAN could replicate where individuals looked, but it modeled only discrete fixation positions and did not simulate continuous eye movements; therefore, it could not capture actual saccadic trajectories or velocity profiles.

In addition to image-conditioned models, multiple research [41–43] investigated stimulus-agnostic approaches to synthesizing eye movement data. Fuhl et al. [41] utilized fully convolutional networks for semantic segmentation, reconstruction, and variational autoencoder (VAE)-based generation of raw eye-tracking data without preprocessing, facilitating arbitrary input dimensions. As it was not conditioned on user identity or task, the generated sequence represented generic behavior averaged over many individuals. Therefore, recent studies have begun incorporating adversarial [23] and diffusion models [25, 44] to produce task-specific eye movements. SP-EyeGAN [24] introduced a GAN-based approach explicitly designed to produce fixations and saccades. DiffGaze [45], a diffusion-based model was introduced to synthesize scanpaths at 30 Hz for 360°VR images. But both, SP-EyeGAN and DiffGaze generates output stimulus-driven behavior without the subject’s identity. Meanwhile, Jiao et al. [26] proposed DiffEyeSyn, the first approach to generate user-specific eye movements. It utilized a conditional diffusion model [46] based on Diffwave [47] that injects personalized noise patterns into a base eye movement sequence, effectively superimposing a user’s unique micro-movement signature onto a generic scanpath.

In our study, we focused on both SP-EyeGAN and DiffEyeSyn. For SP-EyeGAN, we introduced a module to enable it to generate subject-specific gaze sequences. Additionally, for DiffEyeSyn, which employs an identity removal approach, extreme downsampling can overlook mid-frequency data, leading to interpolation problems. It utilizes a pre-trained model’s 512-dimensional user embedding, which increases complexity and may include redundant features. To tackle these issues, we further improve personalized gaze generation by downsampling to a more moderate intermediate frequency (i.e., 25 Hz) and simplifying the identity representation to a single 128-dimensional user embedding, making the conditioning more compact and focused.

3 Implemented Architectures

In this section, we present our customized architectures for both generative approaches, designed to produce subject-specific synthetic eye movement signals. Both architectures inject compact subject information but differ in how they model dynamics. The overall architectures are shown in Figure 1(a) (i.e., DiffEyeSyn) and Figure 1(b) (i.e., SP-EyeGAN).

3.1 DiffEyeSyn

3.1.1 Background

In practice, denoising diffusion probabilistic models (DDPMs) [25] consist of two processes: forward and reverse. In DDPMs, the forward process is a Markov chain that gradually corrupts data with Gaussian noise according to a predefined variance schedule until the data becomes completely noisy. The reverse process, parameterized by a neural network (often a U-Net), learns to invert this corruption by predicting the added noise at each step and iteratively denoising from pure noise back to clean data. In addition, conditional diffusion [46] includes additional features (e.g., subject embeddings or identity-suppressed signals) via feature-wise modulation or cross-attention, and can use classifier-free guidance to balance realism against conditioning strength.

3.1.2 Data Preprocessing

In our task, let the gaze sequence be $p \in \mathbb{R}^{S \times d}$, where S is the number of samples in *milliseconds*(*ms*) and $d = 2$ denotes horizontal and vertical positions. As illustrated in Figure 1(a), p is first fed into the Identity Removal module. In the original pipeline, the 1,000 Hz signal is downsampled to 20 Hz and then upsampled back to 1,000 Hz via interpolation to suppress identity cues. However, building on prior work [27] and our analysis, we instead downsample to 25 Hz and then upsample to 1,000 Hz. According to the Percentage of Variance Accounted For (PVAF) analysis [27], the 0–25 Hz band retains nearly all variance in saccade trajectories (i.e., it preserves signal structure) while diminishing higher-frequency components that convey identity features. Later on, the identity-removed positional signal ($^\circ$) and raw

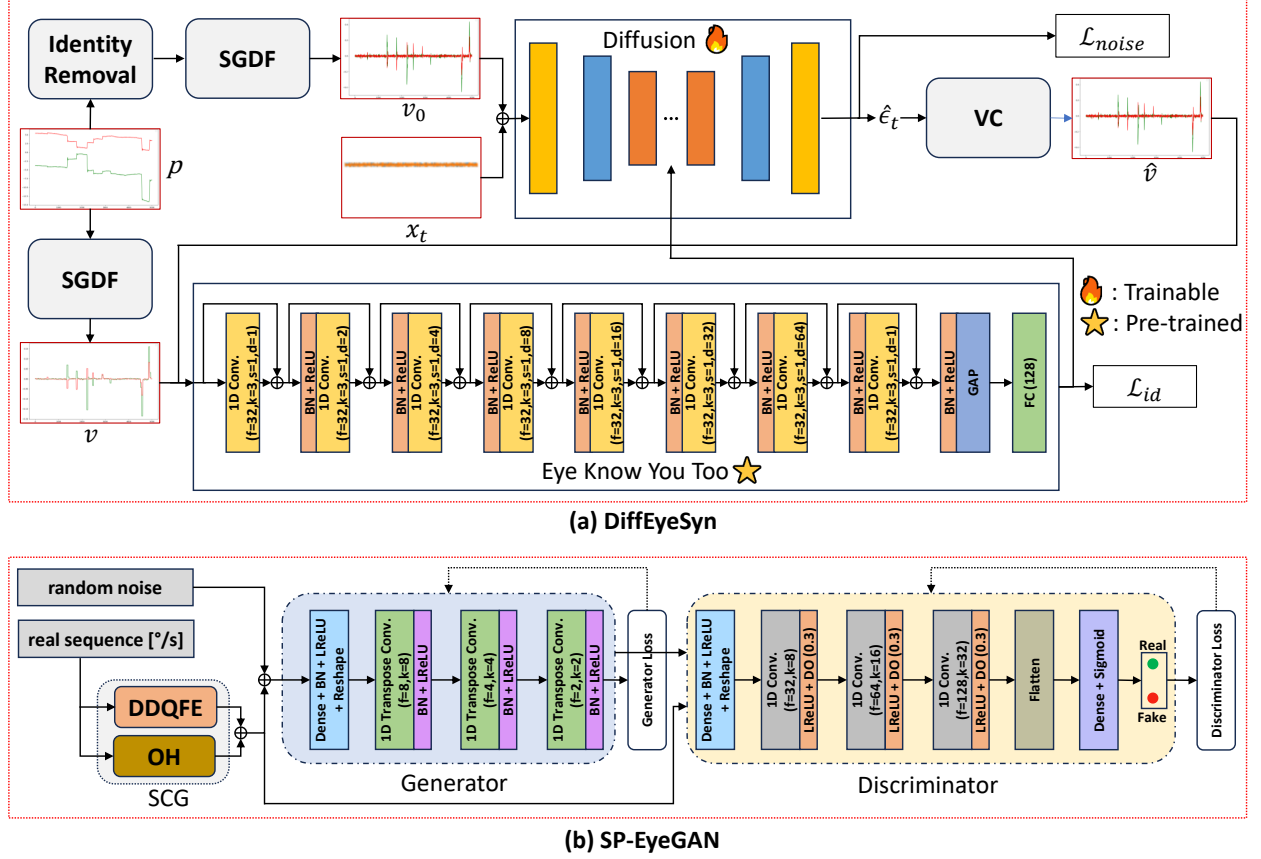


Figure 1: (a) Overview of the updated DiffEyeSyn architecture: The original positional signal p is processed through the Identity Removal module and an SGDF filter to produce an identity-removed velocity v_0 , while using only the SGDF yields the raw velocity v . At each diffusion step t , noise x_t and v_0 serve as input to the diffusion model, which is conditioned on user embeddings from the pre-trained Eye Know You Too encoder. The model predicts noise ($\hat{\epsilon}_t$), which is then converted into the predicted velocity \hat{v} . (b) Overview of the updated SP-EyeGAN architecture: The Subject-Specific Condition Generator (SCG), composed of a DDQFE and a one-hot (OH) encoder, extracts conditional features from the original velocity sequences and metadata. The generator uses random noise and these features to produce synthetic eye movements (fixations or saccades), depending on whether the FixGAN or SacGAN model is used.

positional signals ($^\circ$) are converted into velocity signals (i.e., $^\circ/s$) using the Savitzky-Golay [48] differentiation filter (SGDF) with order 2, deriv 1 and window size 7 as follows:

$$\begin{aligned} v_0 &= \text{SGDF}(\text{IdentityRemoval}(p)), \\ v &= \text{SGDF}(p) \end{aligned} \quad (1)$$

where v is the original velocity signals ($^\circ/s$) and v_0 is the identity-removed velocity signals ($^\circ/s$). Subsequently, invalid velocity samples (e.g., NaNs) are assigned a value of zero, the same as DiffEyeSyn. To mitigate the effect of noise and extraneous spikes, velocities are constrained to the interval $[-1000, 1000]$ $^\circ/s$. The truncated values are then rescaled to the range $[-90, 90]$ and normalized to $[-1, 1]$ using a sine-based transformation, which constrains amplitudes while preserving relative dynamics.

3.1.3 Conditional Diffusion Model

For identity-removed velocity signals v_0 , in the diffusion step t , the noised sample is formed as follows:

$$x_t = \sqrt{\alpha_t} v_0 + \sqrt{1 - \alpha_t} \epsilon_t, \quad \epsilon_t \sim \mathcal{N}(0, I) \quad (2)$$

where x_t is the noisy sample at step t , $\bar{\alpha}_t$ is the cumulative noise-retention factor, ε_t is the Gaussian noise, $\mathcal{N}(0, I)$ is the normal distribution, and $t \in \{1, \dots, T\}$ denotes the number of discrete diffusion time steps (i.e., the length of the forward noising and reverse denoising Markov chain).

Furthermore, to guide the diffusion model in producing genuine subject-specific signals, we employed pre-trained user encoder from Eye Know You Too (EKYT) [7] (i.e., $\phi(\cdot)$), which derives the user embedding (i.e., $z = \phi(v)$) that works as a conditioning factor. EKYT is a DenseNet-based architecture that processes 5 seconds of 1000 Hz eye movement velocity data to derive a 128-dimensional user embedding. Additionally, the original EKYT model was trained using 4-fold cross-validation, yielding 512-dimensional embeddings in DiffeyeSyn. However, we have used a 128-dimensional embedding learned from a single fold of the cross-validation model. Notably, EKYT employs different data processing methodologies. For details, please refer to the EKYT [16] paper. Overall, the smaller vector reduces model capacity and interferes less with the denoising process while still capturing person-dependent traits.

And the noise prediction is performed as follows:

$$\hat{\varepsilon}_t = \varepsilon_\theta(x_t, t, \text{cond}), \quad \text{cond} = (v_0, z), \quad z = \phi(v) \quad (3)$$

where $\varepsilon_\theta(\cdot)$ is the neural network denoiser with parameters θ ; t is the diffusion timestep; cond provides conditioning from the signal (v_0) and user identity (z from the pre-trained encoder $\phi(\cdot)$).

Additionally, after obtaining $\hat{\varepsilon}_t$, this estimate serves as input to the velocity-converter (VC) module, which reconstructs the velocity signals (i.e., \hat{v}) using the following equation:

$$\hat{v} = \frac{x_t - \sqrt{1 - \bar{\alpha}_t} \hat{\varepsilon}_t}{\sqrt{\bar{\alpha}_t}} \quad (4)$$

The model iteratively transforms the noisy sample x_t into a cleaner one x_{t-1} by predicting the noise in x_t , removing it in a way consistent with the forward process. The overall reverse transition is as follows:

$$p_\theta(x_{t-1} | x_t, \text{cond}) = \mathcal{N}(\mu_\theta(x_t, t, \text{cond}), \sigma_t^2 I) \quad (5)$$

where p_θ parameterizes the reverse Markov step; μ_θ is the predicted mean; σ_t^2 is the posterior variance term used for sampling. Overall, At each step t the μ_θ and σ_t^2 can be obtained from:

$$\mu_\theta(x_t, t, \text{cond}) = \frac{1}{\sqrt{\alpha_t}} \left(x_t - \frac{1 - \alpha_t}{\sqrt{1 - \bar{\alpha}_t}} \hat{\varepsilon}_t \right), \quad \sigma_t^2 = \frac{1 - \bar{\alpha}_{t-1}}{1 - \bar{\alpha}_t} (1 - \alpha_t). \quad (6)$$

Finally, each denoising step can be written as:

$$x_{t-1} = \mu_\theta(x_t, t, \text{cond}) + \sigma_t \eta, \quad \eta \sim \mathcal{N}(0, I) \quad (7)$$

Following DiffEyeSyn, we also train the diffusion model using two complementary objectives. The noise-prediction loss (i.e., $\mathcal{L}_{\text{noise}}$) controls the reverse denoising process by reconstructing the Gaussian noise introduced at a timestep t . To maintain subject-specific characteristics, we incorporate the identity-guidance loss (i.e., \mathcal{L}_{id}) that promotes the alignment of the embedding of the generated velocity \hat{v} with the embedding of the user's original velocity v , utilizing the pre-trained encoder $\phi(\cdot)$ and cosine similarity [7]. The overall objective is a weighted sum of these components, with λ controlling the strength of identity guidance. The losses are as follows:

$$\mathcal{L}_{\text{noise}} = \|\varepsilon_t - \hat{\varepsilon}_t\|, \quad (8)$$

$$\mathcal{L}_{\text{id}} = 1 - \cos(\phi(\hat{v}), \phi(v)), \quad (9)$$

$$\mathcal{L} = \mathcal{L}_{\text{noise}} + \lambda \mathcal{L}_{\text{id}} \quad (10)$$

3.2 SP-EyeGAN

3.2.1 Background

Generative adversarial networks (GANs) [23] generate data through an adversarial process that includes a generator, which converts random noise or data into candidate samples, and a discriminator, which learns to distinguish between real and synthetic data. The SP-EyeGAN [24] approach utilizes generators and discriminators for both fixations and saccades, thus enhancing the simulation of scanpath structure. We retain this architecture and make generation explicitly subject- and quality-aware by conditioning with a lightweight Subject-Specific Condition Generator (SCG) module.

3.2.2 Data Preprocessing

Following SP-EyeGAN, we train two identical GANs (i.e., FixGAN and SacGAN) for fixations and saccades, respectively. Raw gaze streams (i.e., 1000 Hz) are first segmented into fixations and saccades using the Dispersion–Threshold Identification (I-DT) algorithm [49]. For each segment, positional samples are converted to 2D velocities ($^{\circ}/s$) using an SGDF [48], and a smoothing technique was employed as in the original SP-EyeGAN. Subsequently, invalid velocity samples (e.g., NaNs) are replaced with 0. The created segments represent two datasets—fixation_dataset and saccade_dataset—used to train the respective GANs.

3.2.3 Subject-Specific Condition Generator

The Subject-Specific Condition Generator (SCG) module comprises two components: the Directional Data Quality Feature Extractor (DDQFE) and the one-hot (OH) encoder. The DDQFE incorporates horizontal and vertical velocities into displacement profiles and derives two metrics per axis: spatial dispersion (i.e., standard deviation) and temporal energy (i.e., root-mean-square error). The resultant feature vector encapsulates fundamental data quality and movement intensity without necessitating an extensive learned embedding. Furthermore, subject identity is represented as an OH representation with a dimensionality equal to the number of training subjects. Thereafter, the features from DDQFE and OH are concatenated together, and this straightforward, fixed representation provides distinct identification conditioning.

3.2.4 Conditional GAN Model

For a given sample from the fixation_dataset $f_v \in \mathbb{R}^{T \times d}$, where T is the number of time steps in ms and $d = 2$ corresponds to the horizontal and vertical velocity components ($^{\circ}/s$). Subject identifiers and other metadata are stored alongside each sample. An equivalent representation is considered for the saccade_dataset. FixGAN generates micro-movements during fixations, while SacGAN simulates the swift dynamics of saccades. The extended conditional architecture of the GAN is illustrated in Figure 1(b).

First, we concatenate the latent noise vector with the features produced by the SCG module. Next, the concatenated vector is passed through a fully connected (Dense) layer, followed by batch normalization (BN) and a LeakyReLU activation. The features are subsequently restructured to conform to the intended sequence lengths of 100 ms for fixations and 30 ms for saccades. Later, this step is followed by three sequential 1D transposed convolution blocks; each block uses a different number of filters f and kernel size k , and is followed by BN and LeakyReLU activation. The final block outputs a two-channel sequence (horizontal and vertical), yielding a synthetic 2D velocity sequence that corresponds to the required temporal resolution.

Meanwhile, the discriminator receives a 2D velocity sequence and necessary metadata and predicts whether it is real or generated. Initially, it has layers similar to those of generators: a dense layer, batch normalization (BN), and a LeakyReLU activation, followed by reshaping the features for the convolutional blocks. Additionally, the discriminator consists of three convolutional blocks, each composed of a convolution and a LeakyReLU, followed by a Flatten and a Dense layer with a sigmoid output. Overall, FixGAN and SacGAN were trained with conditional adversarial losses using binary cross-entropy (BCE). Let c be the conditioning features from the SCG module, f_v be an original 2D velocity sequence, z be latent noise, $G(z, c)$ be the generator output, and $D(\cdot)$ be the discriminator’s probability of being real or fake. The discriminator is set up to give high scores to real conditioned pairings (f_v, c) and low scores to generated pairs ($G(z, c)$). The generator is set up to trick the discriminator. The equations for both losses are as follows:

$$\mathcal{L}_D = \mathbb{E}_{(f_v, c) \sim p_{\text{data}}} [-\log D(x, c)] + \mathbb{E}_{z \sim p(z), c} [-\log(1 - D(G(z, c), c))]. \quad (11)$$

$$\mathcal{L}_G = \mathbb{E}_{z \sim p(z), c} [-\log D(G(z, c), c)]. \quad (12)$$

where \mathcal{L}_D is the binary cross-entropy loss for the discriminator, \mathcal{L}_G is the binary cross-entropy loss for the generator, p_{data} is the real data distribution over pairs (x, c) , and $p(z)$ is the noise prior (e.g., $\mathcal{N}(0, I)$).

Finally, after training FixGAN and SacGAN, we create complete gaze trajectories using fixation and saccade sequences. Following SP-EyeGAN, we first identify n fixation points before building the trajectory by concatenating the fixation segments with saccades. For additional details, please refer to the SP-EyeGAN [24] paper.

4 Experiments

4.1 Dataset

For our experiment, we used the publicly available GazeBase [3] dataset to train and evaluate performance. The complete dataset was collected using the Eyelink 1000 and captured monocular (i.e., left-eye) movement at a rate of 1,000 Hz. Nine rounds were conducted over a 37-month period, involving 322 volunteers and yielding 12,334 eye-tracking records. Specifically, it contains seven tasks: fixation (FXS), horizontal saccade (HSS), random oblique saccade (RAN), reading (TEX), free viewing of cinematic video (VD1 and VD2), and gaze-driven gaming (BLG). Furthermore, among these seven tasks, only RAN and HSS have corresponding stimulus signals that enable the calculation of spatial accuracy and spatial precision metrics. Refer to the GazeBase [3] paper for further information. To utilize the EKYT [7] pre-trained model correctly, we adopted a similar dataset split setting for all six tasks, as BLG was excluded from training. In particular, the training set comprises recordings from the remaining 263 participants. Moreover, the test set includes recordings from 59 subjects who were present in round 6, and in our work, only the first 5 seconds of the signal were evaluated. There was no overlap between users in the training and test sets, ensuring that both the diffusion and GAN-based models’ evaluations were performed on completely unseen users.

4.2 Implementation Details

We trained DiffEyeSyn on 5s windows sampled at 1,000 Hz (5,000 samples per window) using a diffusion process with $T = 50$ and a linear scheduler from 0.0001 to 0.05, where T is the number of discrete diffusion time steps in the forward and reverse processes. Additionally, the Adam optimizer [50] was utilized with a learning rate of 0.0002 and a batch size of 32, and the model was trained for 450 epochs. Meanwhile, SP-EyeGAN was trained for 100 epochs with a batch size of 16 and a learning rate of 0.0001. As the original SP-EyeGAN model was trained only on the TXT stimulus from GazeBase, we trained all the tasks separately, since FixGAN/SacGAN generate fixations and saccades, not the entire signal. All experiments were conducted with Python version 3.9.12, CUDA 12.4, PyTorch 2.1.0, PyTorch-Lightning 1.9.5, and TensorFlow 2.14.0 on two NVIDIA RTX A6000 GPUs (48 GB GDDR6 each). Since DiffEyeSyn has no official publicly available implementation, to ensure reproducibility, we will release the complete source code for both approaches.

5 Results

In this section, we present the metrics for evaluating the quality of synthetic signals [28], including spatial accuracy, spatial precision for error percentile (E), and user percentile (U). For spatial accuracy and spatial precision, we considered stable fixation periods. According to previous study [51], we followed the binning approach, in which, for each signal, we first identified 80-*ms* fixation periods. Later on, these stable bins were used for evaluations.

5.1 Spatial Accuracy

Spatial accuracy was evaluated as the gaze-point error in degrees of visual angle (dva) between the synthetic gaze and the actual target stimulus position. Table 1 presents the spatial accuracy of the ground truth (i.e., the original gaze signal), SP-EyeGAN, and DiffEyeSyn approaches for user (U) and error (E) percentiles. For both tasks, including RAN and HSS, DiffEyeSyn consistently achieves a better score than SP-EyeGAN. For instance, at the median user level (U50), DiffEyeSyn’s E50 (median error) remains relatively low (i.e., 3.73 and 4.06 dva in HSS and RAN). In contrast, SP-EyeGAN’s E50 is higher in RAN (i.e., 13.63 dva) and increases more noticeably for HSS to 15.45 dva. Compared to the ground truth, U50|E50 is not quite satisfactory for both approaches; however, these models were trained to generate synthetic data that tends to resemble the raw signal. Comparing SP-EyeGAN and DiffEyeSyn, the differences indicate that DiffEyeSyn’s signals are closer to ground truth and limit the extreme error outliers. However, for average-case scenarios like (U50|E50) or for the most challenging users or conditions (U95|E95), DiffEyeSyn’s error (i.e., 26.77 dva) is better than that of SP-EyeGAN’s (i.e., 47.07 dva) for RAN. This reliability across different user percentiles means DiffEyeSyn performs more consistently for a broader range of users.

From a practical applications standpoint, these spatial accuracy outcomes have profound implications. Applications that use gaze pointing or foveated rendering often optimize for the median anticipated gaze error to ensure smooth performance under normal conditions. The percentile-centric UIE analysis helps identify these criteria. For instance, consider an application that aims to serve the median user and meet accuracy standards 50% of the time for each user (U50|E50). In that case, the results in Table 1 show that using SP-EyeGAN’s synthetic data would entail accepting a higher median error threshold than DiffEyeSyn. This suggests that interfaces using SP-EyeGAN’s data require larger target sizes or more lenient selection criteria to compensate for its less precise typical performance. Meanwhile,

Table 1: Evaluation of UIE spatial accuracy metrics across different user percentiles for two tasks, including horizontal saccade (HSS) and random oblique saccade (RAN). Here, Ground truth denotes the original positional signal.

Model	U50IE50		U95IE95	
	HSS	RAN	HSS	RAN
Ground truth	0.89	0.92	30.85	21.80
SP-EyeGAN	15.45	13.63	52.73	47.07
DiffEyeSyn	3.73	4.06	38.61	26.77

DiffEyeSyn’s lower median error indicates that gaze-driven interfaces can be made more precise (with smaller targets or narrower margins) in normal use while remaining reliable for average users. However, for worst-case scenarios (U95IE95), both approaches failed to achieve a better score, which denotes that further improvements are needed.

5.2 Spatial Precision

Spatial precision represents the stability of the gaze signal, typically measured as the root mean square (RMS) dispersion of gaze points during steady fixations. We evaluate precision in degrees RMS, with lower values indicating less signal jitter when the user is looking at a fixed point. Table 2 demonstrates the spatial precision for the ground truth (i.e., the original gaze signal), SP-EyeGAN, and DiffEyeSyn. Both approaches achieve similar high precision on average: for the median user (U50), the E50 precision (median jitter) is 0.01 degrees in HSS for SP-EyeGAN and DiffEyeSyn, indicating that, on average, their synthetic gaze remains fairly steady during a fixation. In more demanding tasks, such as RAN, both models exhibit similar jitter due to small fixation instabilities between saccades.

Table 2: Evaluation of UIE spatial precision metrics across different user percentiles for two tasks, including horizontal saccade (HSS) and random oblique saccade (RAN). Here, Ground truth denotes the original positional signal.

Model	U50IE50		U95IE95	
	HSS	RAN	HSS	RAN
Ground truth	0.01	0.01	0.86	1.14
SP-EyeGAN	0.01	0.01	0.37	0.41
DiffEyeSyn	0.01	0.01	0.35	0.29

However, the difference in precision becomes dramatic when looking at the E95 percentile (worst-case scenarios) and higher user percentiles. SP-EyeGAN’s precision increases significantly for the worst-case users/scenarios. At U95IE95, precision error reaches around 0.41 degrees RMS in the RAN task (signifying volatile gaze points for some sequences). DiffEyeSyn, by contrast, manages to constrain the worst-case jitter to 0.29—even the 95th percentile user experiences only moderate RMS noise in DiffEyeSyn’s output. This suggests that a subset of synthetic sequences from SP-EyeGAN suffers from jitter or noise spikes, whereas DiffEyeSyn avoids generating such extreme outliers.

5.3 Synthetic Data Similarity

To evaluate how realistic the synthetic eye movement data are, we computed the cosine similarity between the synthetic sequences and real eye-tracking sequences in a learned feature space. Specifically, we leverage pre-trained EKYT model to extract embeddings and measure the cosine similarity between the embeddings of synthetic and ground-truth sequences. A higher cosine similarity (closer to 1.0) indicates that the synthetic data captures the salient patterns of the real eye movements. As shown in Table 3, we calculated similarity scores for all the tasks. Here, DiffEyeSyn outperforms SP-EyeGAN in similarity across all seven tasks, often by a substantial margin. For example, in the gaze-driven game task (i.e., BLG), which involves complex and idiosyncratic eye movement patterns, DiffEyeSyn achieves a significantly higher cosine similarity score (i.e., 0.94) with real data, indicating that it accurately reproduces the rapid context-dependent gaze shifts of the game. In contrast, SP-EyeGAN’s similarity score is considerably lower (i.e., 0.12), suggesting it struggles to model these irregular patterns. A similar pattern is seen in simpler behaviors as well: even for FXS and HSS, DiffEyeSyn yields similarity scores close to the actual embeddings—0.92 for both—outperforming SP-EyeGAN’s 0.08 and 0.05 scores. Notably, even in TEX—the task for which the original SP-EyeGAN was trained—DiffEyeSyn’s synthetic gaze sequences better match real reading patterns with 0.95 similarity scores.

Table 3: Cosine similarity between pre-trained EKYT embeddings of real and synthetic eye movement data for SP-EyeGAN and DiffEyeSyn.

Model	BLG	FXS	HSS	RAN	TEX	VD1	VD2
SP-EyeGAN	0.12	0.08	0.05	0.03	0.07	0.05	0.05
DiffEyeSyn	0.94	0.92	0.92	0.95	0.95	0.95	0.92

In general, these results indicate that DiffEyeSyn can accurately reproduce a wide range of eye movement dynamics. In practical terms, higher synthetic–real similarity indicates a more effective use of synthetic data. For example, DiffEyeSyn’s synthetic eye sequences behave more like real eye movement data and can be used to simulate how people behave in AR/VR testing, thereby closing the gap between simulation and reality. Conversely, SP-EyeGAN’s lower similarity across several tasks suggests that it may overlook important aspects of gaze behavior. Despite this, we trained SP-EyeGAN with subject-guided additional conditioning, generating fixations and saccades separately and then combining them into complete gaze sequences. This approach appears less effective for the user authentication task, as indicated by a lower similarity score. Finally, DiffEyeSyn’s synthetic gaze’s superior score provides a pathway for the AR/VR domain by utilizing synthetic eye movement data to match real data with minimal compromise.

5.4 Qualitative Evaluations

Figure 2 represents the comparison of raw eye-tracking signals to synthetic signals generated by SP-EyeGAN and DiffEyeSyn across two representative tasks for both gaze position and velocity. In visual inspection, for both tasks in Figure 2(a), (b), both approaches produce qualitatively plausible eye movement sequences; however, DiffEyeSyn produces more accurate, human-like signals than SP-EyeGAN. In particular, DiffEyeSyn’s synthetic sequences more closely follow the ground truth patterns—exhibiting smoother velocity shapes with less jitter and more well-aligned fixation and saccade segments. This improvement is due to the way DiffEyeSyn is customized: its conditional diffusion model and subject-specific, lightweight user embeddings enable it to capture subtle subjective dynamics in eye movement data, resulting in synthetic signals that are more like the real ones.

6 Discussion

6.1 Interpreting Visual Quality Findings

By utilizing generative models like diffusion and GANs, achieving a signal quality entirely similar to the ground truth is challenging, as a perfect gaze movement signal should contain similar saccades, fixations, amplitudes, and other characteristics. As shown in Figure 2, all the signals of DiffEyeSyn appear to be close to the ground truth signals. However, a close inspection reveals that the horizontal signal in Figure 2(a) at 1000 *ms*, DiffEyeSyn, contains an extra microsaccade before a fixation, which is not present in the ground truth signal. Meanwhile, SP-EyeGAN attempts to follow the ground truth, but it lags and fails to generate corresponding fixations and saccades.

Similar issues occur in the RAN task (i.e., Figure 2(b)). Here, SP-EyeGAN’s outputs exhibit apparent mismatches: the synthetic sequences have incorrect saccade counts and fixation durations, with additional saccades and shorter, less stable fixations than those in the real data for both horizontal and vertical signals. The gaze position traces from SP-EyeGAN fluctuate during intervals where the real eye remains steady, and their fixations show unnatural drift. Additionally, the gaze velocity plots reveal spurious high-velocity spikes that are absent in the real signals. Even DiffEyeSyn generates gaze signals that contain extra saccades before some fixations. More specifically, in the vertical signal of Figure 2(b), after 2000 *ms*, there is an extra saccade, whereas in the ground truth signal, it is relatively smooth. This indicates that DiffEyeSyn failed to produce the expected near-static fixation pattern; instead, it generates a different sequence with a false saccade, resulting in a velocity profile with a noticeable spike. These differences suggest that further research and model improvements are necessary to achieve the optimal accuracy in synthetic eye movement signals.

6.2 Synthetic Data Quality and Subject Specificity

We have reintroduced subject-specific SP-EyeGAN and DiffEyeSyn that generate realistic gaze movement signals. As proof of the effectiveness of synthetic signals, we have demonstrated spatial accuracy, precision, and cosine similarity with real data embeddings. From Tables 1, 2, and 3, the results indicate that DiffEyeSyn with compact conditioning provides a more faithful output of individual gaze dynamics than the adversarial baseline. The combination of identity-removed guidance (i.e., 25 Hz) and a 128-dimensional subject embedding improves spatial accuracy/precision while strengthening subject alignment, suggesting that smaller, more invariant identity features reduce interference during



Figure 2: Qualitative comparison between SP-EyeGAN and DiffEyeSyn for two different tasks: (a) TEX and (b) RAN. For each task, the first row contains the positional signal, and the second row contains the velocity signal.

denoising. By contrast, the subject-aware SP-EyeGAN—augmented with DDQFE cues and OH features—improves over its original form but still lags behind DiffEyeSyn, particularly in terms of temporal fidelity and spectral similarity. From Figure 2, qualitatively, the diffusion-based approach produces smoother velocity shapes, cleaner fixation plateaus, and more realistic saccadic onset/offset kinematics, whereas the GAN-based approach occasionally exhibits jitter and underestimates peak velocities.

Additionally, the performance scores across user and error (UIE) percentiles in Tables 1 and 2 highlight practically relevant trade-offs in gaze-tracking signal quality. This analysis of synthetic data shows that designing applications for a specific range of users and conditions makes AR/VR interactions easier to use and more reliable. DiffEyeSyn maintains relatively good spatial accuracy (i.e., 3.73 and 4.06 dva), indicating that during median (i.e., U50IE50 for HSS and RAN), its output remains more reliable than SP-EyeGAN, which has 15.45 and 13.63 dva.

6.3 Data Efficiency and Privacy Considerations

A significant concern in subject-specific gaze synthesis is minimizing reliance on large-scale real datasets while mitigating privacy exposure. Our findings demonstrate that compact identity conditioning, combined with identity-suppressed guidance, enables the generation of high-fidelity, subject-aware gaze sequences from relatively modest real-world data inputs. However, pipelines incorporating subject-specific signals pose residual risks of feature leakage or re-identification if not adequately constrained. Because DiffEyeSyn and SP-EyeGAN depend on user embeddings for generating subject-specific signals and on subjects’ metadata, respectively, we consider this research a step toward privacy-preserving synthetic augmentation, where not raw signals but rather embeddings and metadata will be used.

6.4 Limitations and Future Directions

This study focuses on generating subject-guided, high-frequency, lab-grade gaze movement sequences, which opens the pathway to extending performance to lower-fidelity consumer devices. Currently, the model is highly dependent on proper training on a large-scale dataset and requires multiple preprocessing steps. Additionally, both approaches, including SP-EyeGAN and DiffEyeSyn, require subject-specific features as a condition. The current identity-removing mechanism in DiffEyeSyn (i.e., downsample–upsample) may introduce minor distortions; future architectures could benefit from end-to-end learned guidance or signal-specific low-pass filters. Furthermore, utilizing a single diffusion process to incorporate self-supervised or task-adaptive embeddings, and including explicit conditioning tokens (e.g., task, stimulus), represents key avenues for expanding control and generalization in subject-specific gaze synthesis.

7 Conclusion

In this work, we have customized two generative models to generate synthetic gaze movements under subject-specific conditions. More specifically, we have employed SP-EyeGAN and added subject-identity features using the Subject-Specific Condition Generator (SCG) module. Additionally, we customized the DiffEyeSyn approach to generate more realistic modalities. Furthermore, we have conducted a head-to-head comparison of both GANs and diffusion-based approaches in terms of spatial accuracy, precision, and cosine similarity metrics, where DiffEyeSyn outperforms SP-EyeGAN by a larger margin. Finally, DiffEyeSyn produces more meaningful spatial accuracy and precision metrics; visual inspection indicates that the synthetic data closely matches the real one.

Privacy and Ethics Statement

This study uses anonymized, publicly available eye-tracking data to train generative models, posing minimal societal risk. No personal data was used, and we encourage responsible application to avoid potential misuse. Our work supports ethical, privacy-conscious advancements in eye-tracking research.

References

- [1] Hong Fu, Ying Wei, Francesco Camastra, Pietro Arico, and Hong Sheng. Advances in eye tracking technology: theory, algorithms, and applications. *Computational intelligence and neuroscience*, 2016:7831469, 2016.
- [2] Xin Jin, Suyu Chai, Jie Tang, Xianda Zhou, and Kai Wang. Eye-tracking in ar/vr: A technological review and future directions. *IEEE Open Journal on Immersive Displays*, 2024.
- [3] Henry Griffith, Dillon Lohr, Evgeny Abdulin, and Oleg Komogortsev. Gazebase, a large-scale, multi-stimulus, longitudinal eye movement dataset. *Scientific Data*, 8(1):184, 2021.
- [4] Martin Meißner and Josua Oll. The promise of eye-tracking methodology in organizational research: A taxonomy, review, and future avenues. *Organizational Research Methods*, 22(2):590–617, 2019.
- [5] Patrick Haller, Andreas Säuberli, Sarah Elisabeth Kiener, Jinger Pan, Ming Yan, and Lena Jäger. Eye-tracking based classification of mandarin chinese readers with and without dyslexia using neural sequence models. *arXiv preprint arXiv:2210.09819*, 2022.
- [6] Tamilvizhi Thanarajan, Youseef Alotaibi, Surendran Rajendran, and Krishnaraj Nagappan. Eye-tracking based autism spectrum disorder diagnosis using chaotic butterfly optimization with deep learning model. *Computers, Materials & Continua*, 76(2), 2023.
- [7] Dillon Lohr and Oleg V Komogortsev. Eye know you too: Toward viable end-to-end eye movement biometrics for user authentication. *IEEE Transactions on Information Forensics and Security*, 17:3151–3164, 2022.

- [8] Dillon Lohr, Michael J Proulx, Mehedi Hasan Raju, and Oleg V Komogortsev. Gaze authentication: Factors influencing authentication performance. *arXiv preprint arXiv:2509.10969*, 2025.
- [9] Oleg V Komogortsev. Person identification using ocular biometrics with liveness detection, July 14 2015. US Patent 9,082,011.
- [10] Mehedi Hasan Raju, Dillon J Lohr, and Oleg Komogortsev. Iris print attack detection using eye movement signals. In *2022 Symposium on Eye Tracking Research and Applications*, pages 1–6, 2022.
- [11] Anjul Patney, Marco Salvi, Joohwan Kim, Anton Kaplanyan, Chris Wyman, Nir Benty, David Luebke, and Aaron Lefohn. Towards foveated rendering for gaze-tracked virtual reality. *ACM Transactions On Graphics (TOG)*, 35(6):1–12, 2016.
- [12] Raphael Menges, Chandan Kumar, and Steffen Staab. Improving user experience of eye tracking-based interaction: Introspecting and adapting interfaces. *ACM Transactions on Computer-Human Interaction (TOCHI)*, 26(6):1–46, 2019.
- [13] Stephen Hutt, Kristina Krasich, James R. Brockmole, and Sidney K. D’Mello. Breaking out of the lab: Mitigating mind wandering with gaze-based attention-aware technology in classrooms. In *Proceedings of the 2021 CHI conference on human factors in computing systems*, pages 1–14, 2021.
- [14] Benedikt V Ehinger, Katharina Groß, Inga Ibs, and Peter König. A new comprehensive eye-tracking test battery concurrently evaluating the pupil labs glasses and the eyelink 1000. *PeerJ*, 7:e7086, 2019.
- [15] Corey D Holland and Oleg V Komogortsev. Biometric verification via complex eye movements: The effects of environment and stimulus. In *2012 IEEE Fifth International Conference on Biometrics: Theory, Applications and Systems (BTAS)*, pages 39–46. IEEE, 2012.
- [16] Dillon Lohr, Henry Griffith, and Oleg V Komogortsev. Eye know you: Metric learning for end-to-end biometric authentication using eye movements from a longitudinal dataset. *IEEE Transactions on Biometrics, Behavior, and Identity Science*, 4(2):276–288, 2022.
- [17] Chuhan Jiao, Zhiming Hu, Mihai Băce, and Andreas Bulling. Supreyes: Super resolution for eyes using implicit neural representation learning. In *Proceedings of the 36th Annual ACM Symposium on User Interface Software and Technology*, pages 1–13, 2023.
- [18] Sultan Daud Khan and Habib Ullah. A survey of advances in vision-based vehicle re-identification. *Computer Vision and Image Understanding*, 182:50–63, 2019.
- [19] Julian Steil, Inken Hagedstedt, Michael Xuelin Huang, and Andreas Bulling. Privacy-aware eye tracking using differential privacy. In *Proceedings of the 11th ACM Symposium on Eye Tracking Research & Applications*, pages 1–9, 2019.
- [20] Yintong Liu, U Rajendra Acharya, and Jen Hong Tan. Preserving privacy in healthcare: A systematic review of deep learning approaches for synthetic data generation. *Computer Methods and Programs in Biomedicine*, 260:108571, 2025.
- [21] Sooha Park Lee, Jeremy B Badler, and Norman I Badler. Eyes alive. In *Proceedings of the 29th annual conference on Computer graphics and interactive techniques*, pages 637–644, 2002.
- [22] Guohao Lan, Tim Scargill, and Maria Gorlatova. Eyesyn: Psychology-inspired eye movement synthesis for gaze-based activity recognition. In *2022 21st ACM/IEEE international conference on information processing in sensor networks (IPSN)*, pages 233–246. IEEE, 2022.
- [23] Ian Goodfellow, Jean Pouget-Abadie, Mehdi Mirza, Bing Xu, David Warde-Farley, Sherjil Ozair, Aaron Courville, and Yoshua Bengio. Generative adversarial networks. *Communications of the ACM*, 63(11):139–144, 2020.
- [24] Paul Prasse, David Robert Reich, Silvia Makowski, Seoyoung Ahn, Tobias Scheffer, and Lena A Jäger. Sp-eyegan: Generating synthetic eye movement data with generative adversarial networks. In *Proceedings of the 2023 symposium on eye tracking research and applications*, pages 1–9, 2023.
- [25] Jonathan Ho, Ajay Jain, and Pieter Abbeel. Denoising diffusion probabilistic models. *Advances in neural information processing systems*, 33:6840–6851, 2020.
- [26] Chuhan Jiao, Guanhua Zhang, Yeonjoo Cho, Zhiming Hu, and Andreas Bulling. Diffeyesyn: Diffusion-based user-specific eye movement synthesis. *arXiv preprint arXiv:2409.01240*, 2024.
- [27] Mehedi H Raju, Lee Friedman, Troy M Bouman, and Oleg V Komogortsev. Determining which sine wave frequencies correspond to signal and which correspond to noise in eye-tracking time-series. *Journal of Eye Movement Research*, 14(3):16, 2021.

- [28] Samantha Aziz, Dillon J Lohr, Lee Friedman, and Oleg Komogortsev. Evaluation of eye tracking signal quality for virtual reality applications: A case study in the meta quest pro. In *Proceedings of the 2024 Symposium on Eye Tracking Research and Applications*, pages 1–8, 2024.
- [29] Andrew T Duchowski and Sophie Jörg. Modeling physiologically plausible eye rotations. In *Proceedings of computer graphics international*, 2015.
- [30] Andrew T Duchowski, Sophie Jörg, Tyler N Allen, Ioannis Giannopoulos, and Krzysztof Krejtz. Eye movement synthesis. In *Proceedings of the ninth biennial ACM symposium on eye tracking research & applications*, pages 147–154, 2016.
- [31] Xiaohan Ma and Zhigang Deng. Natural eye motion synthesis by modeling gaze-head coupling. In *2009 IEEE Virtual Reality Conference*, pages 143–150. IEEE, 2009.
- [32] Erroll Wood, Tadas Baltrusaitis, Xucong Zhang, Yusuke Sugano, Peter Robinson, and Andreas Bulling. Rendering of eyes for eye-shape registration and gaze estimation. In *Proceedings of the IEEE international conference on computer vision*, pages 3756–3764, 2015.
- [33] Binh H Le, Xiaohan Ma, and Zhigang Deng. Live speech driven head-and-eye motion generators. *IEEE transactions on visualization and computer graphics*, 18(11):1902–1914, 2012.
- [34] Wolfgang Fuhl and Enkelejda Kasneci. Eye movement velocity and gaze data generator for evaluation, robustness testing and assess of eye tracking software and visualization tools. *arXiv preprint arXiv:1808.09296*, 2018.
- [35] Wolfgang Fuhl, Thiago Santini, Thomas Kuebler, Nora Castner, Wolfgang Rosenstiel, and Enkelejda Kasneci. Eye movement simulation and detector creation to reduce laborious parameter adjustments. *arXiv preprint arXiv:1804.00970*, 2018.
- [36] Sang Hoon Yeo, Martin Lesmana, Debanga R Neog, and Dinesh K Pai. Eyecatch: Simulating visuomotor coordination for object interception. *ACM Transactions on Graphics (TOG)*, 31(4):1–10, 2012.
- [37] Greg Welch, Gary Bishop, et al. An introduction to the kalman filter. 1995.
- [38] Daniel Simon, Srinivas Sridharan, Shagan Sah, Raymond Ptucha, Chris Kanan, and Reynold Bailey. Automatic scanpath generation with deep recurrent neural networks. In *Proceedings of the ACM symposium on applied perception*, pages 130–130, 2016.
- [39] Marc Assens, Xavier Giro-i Nieto, Kevin McGuinness, and Noel E O’Connor. Pathgan: Visual scanpath prediction with generative adversarial networks. In *Proceedings of the European Conference on Computer Vision (ECCV) Workshops*, pages 0–0, 2018.
- [40] Harsimran Kaur and Roberto Manduchi. Eyegan: Gaze-preserving, mask-mediated eye image synthesis. In *Proceedings of the IEEE/CVF Winter Conference on Applications of Computer Vision*, pages 310–319, 2020.
- [41] Wolfgang Fuhl, Yao Rong, and Enkelejda Kasneci. Fully convolutional neural networks for raw eye tracking data segmentation, generation, and reconstruction. In *2020 25th International Conference on Pattern Recognition (ICPR)*, pages 142–149. IEEE, 2021.
- [42] Celso M De Melo, Antonio Torralba, Leonidas Guibas, James DiCarlo, Rama Chellappa, and Jessica Hodgins. Next-generation deep learning based on simulators and synthetic data. *Trends in cognitive sciences*, 26(2):174–187, 2022.
- [43] Wolfgang Fuhl and Enkelejda Kasneci. Hpcgen: Hierarchical k-means clustering and level based principal components for scan path generation. In *2022 Symposium on Eye Tracking Research and Applications*, pages 1–7, 2022.
- [44] Alexander Quinn Nichol and Prafulla Dhariwal. Improved denoising diffusion probabilistic models. In *International conference on machine learning*, pages 8162–8171. PMLR, 2021.
- [45] Chuhan Jiao, Yao Wang, Guanhua Zhang, Mihai Băce, Zhiming Hu, and Andreas Bulling. Diffgaze: A diffusion model for modelling fine-grained human gaze behaviour on 360° images. *ACM Transactions on Interactive Intelligent Systems*, 2025.
- [46] Lvmin Zhang, Anyi Rao, and Maneesh Agrawala. Adding conditional control to text-to-image diffusion models. In *Proceedings of the IEEE/CVF international conference on computer vision*, pages 3836–3847, 2023.
- [47] Zhifeng Kong, Wei Ping, Jiaji Huang, Kexin Zhao, and Bryan Catanzaro. Diffwave: A versatile diffusion model for audio synthesis. *arXiv preprint arXiv:2009.09761*, 2020.
- [48] Abraham Savitzky and Marcel JE Golay. Smoothing and differentiation of data by simplified least squares procedures. *Analytical chemistry*, 36(8):1627–1639, 1964.

- [49] Dario D Salvucci and Joseph H Goldberg. Identifying fixations and saccades in eye-tracking protocols. In *Proceedings of the 2000 symposium on Eye tracking research & applications*, pages 71–78, 2000.
- [50] D. P. Kingma and J. Ba. Adam: A method for stochastic optimization. *CoRR*, abs/1412.6980, 2014.
- [51] Dillon J Lohr, Lee Friedman, and Oleg V Komogortsev. Evaluating the data quality of eye tracking signals from a virtual reality system: Case study using smi’s eye-tracking htc vive. *arXiv preprint arXiv:1912.02083*, 2019.